ChemPubSoc Europe

DOI: 10.1002/chem.201504100

CHEMISTRY A European Journal Communication

Self-Assembly

In Situ Visualization of Block Copolymer Self-Assembly in Organic Media by Super-Resolution Fluorescence Microscopy

Charlotte E. Boott,[a] Romain F. Laine,[b] Pierre Mahou,[b] John R. Finnegan,[a] Erin M. Leitao,[a] Stephen E. D. Webb,*[c] Clemens F. Kaminski,*[b] and Ian Manners*[a]

Abstract: Analytical methods that enable visualization of nanomaterials derived from solution self-assembly processes in organic solvents are highly desirable. Herein, we demonstrate the use of stimulated emission depletion microscopy (STED) and single molecule localization microscopy (SMLM) to map living crystallization-driven block copolymer (BCP) self-assembly in organic media at the sub-diffraction scale. Four different dyes were successfully used for single-colour super-resolution imaging of the BCP nanostructures allowing micelle length distributions to be determined in situ. Dual-colour SMLM imaging was used to measure and compare the rate of addition of red fluorescent BCP to the termini of green fluorescent seed micelles to generate block comicelles. Although well-established for aqueous systems, the results highlight the potential of super-resolution microscopy techniques for the interrogation of self-assembly processes in organic media.

The solution self-assembly of block copolymers (BCPs) has enabled the formation of a wide range of micellar nanostructures with a variety of applications from drug delivery to composite reinforcement.[1–6] A challenge associated with the characterization of BCP nanostructures is that current analysis techniques either provide ensemble measurements (e.g. static light scattering), have limited resolution (e.g. laser scanning confocal microscopy (LSCM)), or require the invasive removal of solvent prior to imaging (e.g., electron microscopy).[7] There is, therefore, a compelling need for simple analytical methods that enable visualization of BCP assemblies and analogous nanostructures derived from other self-assembly processes in their native solvent.

Super-resolution fluorescence microscopy techniques such as structured illumination microscopy (SIM),[8] stimulated emission depletion microscopy (STED)[9,10] and single-molecule localization microscopy (SMLM)[9,11–15] have recently emerged as powerful tools to visualize biological structures at the nanometre scale. In particular, self-assembly processes in aqueous media such as protein aggregation[16,17] or more recently formation of synthetic supramolecular fibrils[18] were successfully observed using super-resolution microscopy. In this communication, we illustrate the use of super-resolution fluorescence microscopy for the interrogation of self-assembly processes in organic media, which are also of broad interest.

In the present work we focused on BCP nanostructures formed by living crystallization-driven self-assembly (CDSA), a recently established synthetic approach for the preparation of BCP nanoparticles with precisely controlled size and shape.[19–22] For example, if molecularly dissolved BCP unimers containing a crystallizable core-forming block are added to cylindrical seed micelles derived from the same BCP in a selective solvent for the corona-forming block, this leads to micelle growth from the crystalline core termini (Figure 1 a). This allows access to monodisperse cylinders with a length determined by the unimer to seed ratio.[20] Moreover, addition of a BCP unimer with a different corona-forming block to that of the seed micelles yields block comicelles with spatially separated regions of differing coronal chemistry.[19,21] Living CDSA has been observed for a variety of BCPs with crystallizable segments[23–25] and also, more recently, for planar molecules[26–31] that form supramolecular polymers through π-stacking or hydrogen-bonding interactions. We present here the application of STED and SMLM for the observation and quantitative analysis of micelles formed by living CDSA in their native solvent using fluorescently labelled poly(ferrocenyldimethylsilane) (PFS) BCPs. We compare the micelle length data obtained for the fluorescent PFS cylindrical micelles in solution by super-resolution microscopy techniques with those obtained by TEM on dried samples. In addition, dual-colour SMLM is used to investigate the micelle growth from the termini of cylindrical seed micelles and block comicelle formation.

[a] C. E. Boott, J. R. Finnegan, Dr. E. M. Leitao, Prof. I. Manners
School of Chemistry, University of Bristol
Bristol, BS8 1TS (UK)
E-mail: ian.manners@bristol.ac.uk

[b] Dr. R. F. Laine,[+] Dr. P. Mahou,[+] Prof. C. F. Kaminski
Department of Chemical Engineering and Biotechnology
University of Cambridge, Cambridge, CB2 3RA (UK)
E-mail: cfk23@cam.ac.uk

[c] Dr. S. E. D. Webb
Central Laser Facility, Science and Technology Facilities Council
Research Complex at Harwell, Rutherford Appleton Laboratory
Didcot, OX11 0QX (UK)
E-mail: stephen.webb@stfc.ac.uk

[+] These authors contributed equally.

Supporting information for this article is available on the WWW under http://dx.doi.org/10.1002/chem.201504100.

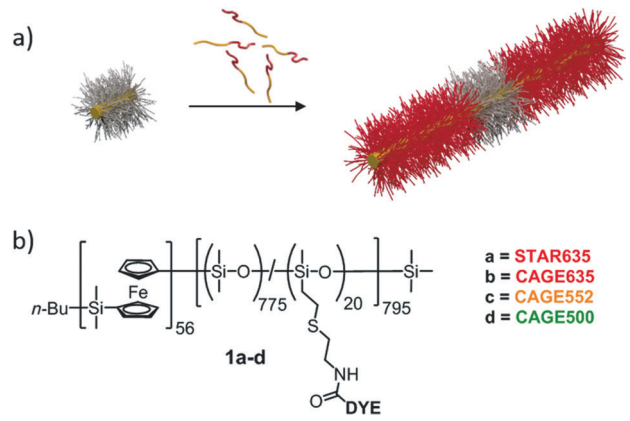

Figure 1. Fluorescent cylindrical micelles of PFS_{56}-*b*-$PDMS_{775}/DYE_{20}$. a) Schematic representation of the formation of fluorescent cylindrical micelles by seeded growth from a non-fluorescent seed (not to scale); yellow = PFS core, red = fluorescent corona, grey = non-fluorescent corona. b) Chemical structure of PFS_{56}-*b*-$PDMS_{775}/DYE_{20}$, showing the position of the fluorescent dyes (DYE).

The successful application of super-resolution imaging by STED and SMLM depends on the selection of fluorescent probes that meet the strict requirements imposed by the two techniques. In general, STED requires highly photostable dyes whilst SMLM needs dye molecules with controllable photoswitching behaviour. For SMLM imaging, there are several ways to induce controllable photoswitching of the dyes. A widely used approach is to add reducing agents such as thiols to common fluorescent probes to turn the fluorescent dyes into a long-lived dark state, a technique called *d*STORM.[14] However, these additives were incompatible with our solvent conditions. Moreover, the properties of the dyes are often solvent dependent and in the present in situ study, dyes soluble in common solvents for the BCP PFS_{56}-b-$PDMS_{775}/DYE_{20}$ (Figure 1 b; PDMS = polydimethylsiloxane) for example, THF, CH_2Cl_2 or chloroform were required. Therefore, to label the BCPs we identified four candidates, all derivatives of rhodamine dyes; STAR635 and CAGE635 for STED, and CAGE635, CAGE552 and CAGE500 for SMLM.[32,33] CAGE dyes were selected for SMLM imaging as they are non-fluorescent in their initial caged state but when exposed to UV light, in the presence of a protic solvent, undergo a Wolff rearrangement that results in the uncaged, fluorescent state. This process is compatible with our organic solvent system.[33]

The BCPs PFS_{56}-*b*-($PDMS_{775}/DYE_{20}$) (Figure 1 b) were prepared from the reaction of a BCP functionalized with pendant amine groups and the *N*-hydroxysuccinimidyl (NHS) ester dyes.[34] Solutions of cylindrical micelles with a crystalline PFS core (BCPs **1 a**–**d**) were prepared with low length polydispersities (PDI) (PDI = L_w/L_n, in which L_w and L_n are the weight and number average micelle lengths, respectively) using a seeded growth living CDSA approach (see Figure 1 a and the Supporting Information for further details).

STED microscopy was performed on cylindrical micelles labelled with STAR635 and CAGE635 dyes using an excitation wavelength of 640 nm and a depletion wavelength of 765 nm (Figure 2). In the case of the CAGE635 dye no additional beam was required for uncaging as it was performed directly by two photon excitation from the STED beam (see the Supporting Information and ref. [33]). For both dyes, cross-sections of the micelles (Figure 2) illustrate the reduction in the micelle widths achieved using STED compared to LSCM, reaching a final mi-

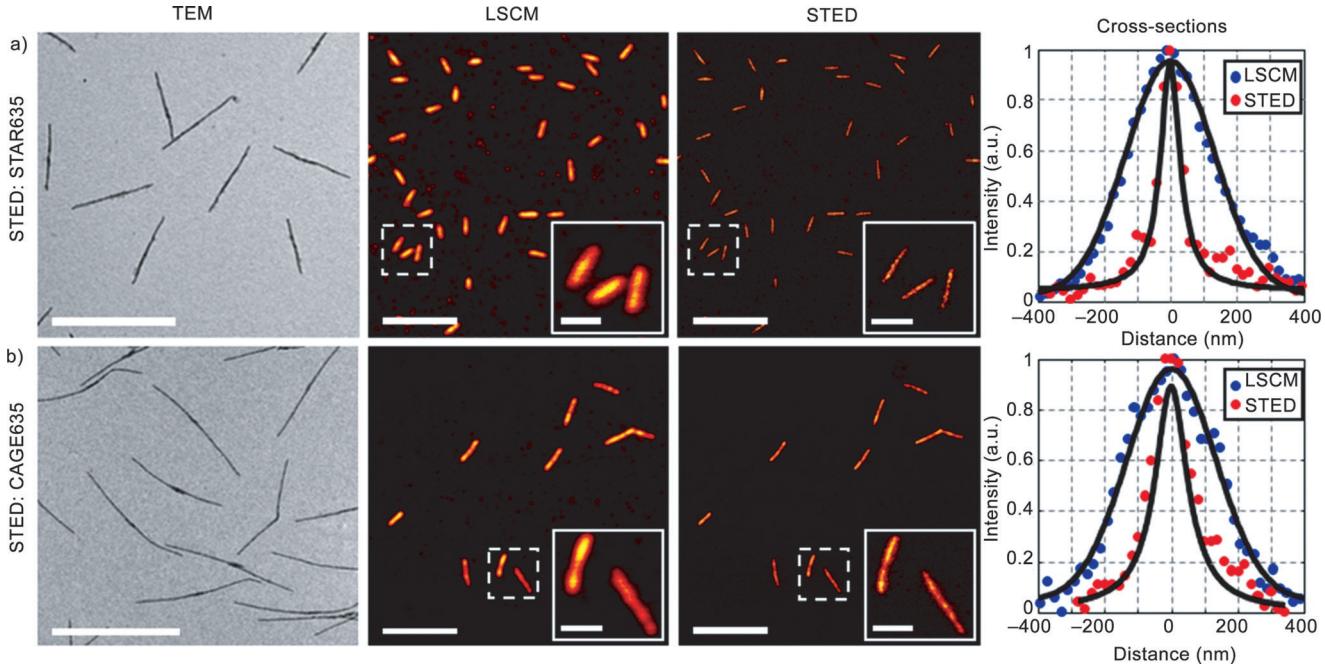

Figure 2. TEM, LSCM and STED images of cylindrical micelles labelled with STAR635 (a) and CAGE635 (b). All acquisitions were performed in native solvent; ethyl acetate for STAR635 and hexane for CAGE635. The uncaging of CAGE635 was performed by two-photon excitation from the STED beam. TEM scale bars: 2000 nm, LSCM and STED scale bars: 5000 nm, inset scale bars: 1000 nm.

celle full-width half-maximum (FWHM) of 77 nm for the dye STAR635.

For SMLM imaging, CAGE635, CAGE552 and CAGE500 dyes were investigated. The labelled cylindrical micelles were all grown in hexane and for imaging 5% isopropanol was added to induce the Wolff rearrangement necessary for the uncaging. The results obtained for CAGE552 are shown in Figure 3a (for other single colour images see the Supporting Information, Figure S4). As shown in Figure 3a, the resolution improvement from wide-field microscopy to SMLM is demonstrated by the reduction in FWHM from 383 to 76 nm, respectively. In order to investigate the micelle growth at both seed termini, dual-colour SMLM was performed on Red-Green-Red (RGR) triblock comicelles in which the middle segment was labelled with CAGE500 and the two outer segments were labelled with CAGE635 (see representative image in Figure 3b). This dye

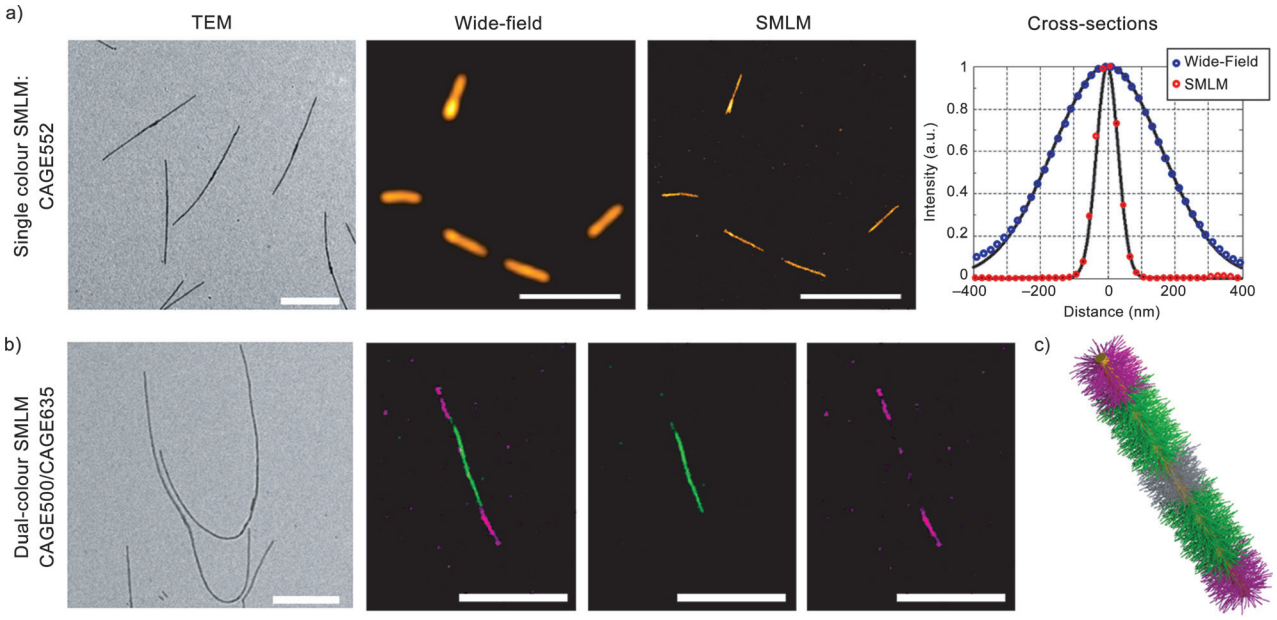

Figure 3. TEM, Wide-field and SMLM images of cylindrical micelles. Single-colour SMLM of cylindrical micelles labelled with the dyes a) CAGE552 and dual-colour imaging of RGR triblock comicelles using b) CAGE500 (green channel) and CAGE635 (red channel), 34 nm non-fluorescent seed could not be resolved. TEM scale bars: 1000 nm Wide-field and SMLM scale bars a) 5000 nm, b) 2000 nm c) Schematic representation of RGR triblock micelle (not to scale)

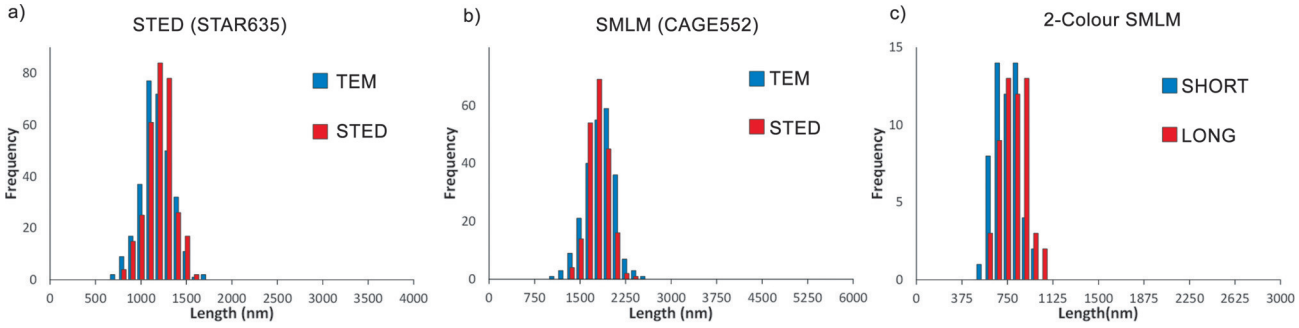

d)

	STED (STAR635)		SMLM (CAGE552)		2-Colour SMLM	
	STED	TEM	SMLM	TEM	SHORT	LONG
L_n (nm)	1153	1121	1724	1752	708	766
L_w (nm)	1172	1146	1742	1784	724	782
PDI	1.02	1.02	1.01	1.02	1.02	1.02
N	312	310	206	235	55	55
σ (nm)	148	167	175	236	107	108

Figure 4. Quantitative analysis of micelle lengths by super-resolution microscopy and TEM counted using hand-tracing method. a–c) Histograms of micelle contour lengths d) Table comparing micelle length data. PDI = L_w/L_n, in which L_w and L_n are the weight and number average micelle lengths, respectively, and σ is the standard deviation.

pairing was selected in order to prevent spectral overlap between the excitation and emission spectra of the dyes.

The micelle length distribution was investigated from the single-colour super-resolution images (Figure 4 and Figure S4, Supporting Information). Our results show that for both super-resolution techniques and the four dyes investigated, the lengths measured by hand and automated tracing (Tables S1, S2 and S4, Supporting Information) are in good agreement with those obtained by TEM (Figure 4 and Figures S5, S7 and S8, Supporting Information).

Finally, we analysed our dual-colour SMLM images of RGR triblock comicelles to gain insight into the relative growth rate of unimer from the cylindrical micelle termini. We extracted the length of the "short" and the "long" segments obtained from the images of CAGE635 acquired by SMLM (Figure 4c and d). We observed that the growth from the termini of the micelles is equivalent in both directions within experimental error. The total lengths of the RGR blocks and the lengths of the seeds were also extracted for comparison between SMLM and TEM (see Table S4 and Figure S8, Supporting Information), and in all cases, the lengths were found to be in good agreement between the two techniques.

In summary, we demonstrate the feasibility of super-resolution imaging (STED and SMLM) in organic media and the substantial resolution improvements over standard fluorescence microscopy techniques. We note that the resolution improvement achieved here with our home-built systems could be further improved through various optimizations. However, ultimately the resulting apparent micelle widths will be limited by the sample width and the precision of the length estimation will be limited by the signal-to-noise ratio of the images, directly impacted by the dye brightness, labelling density and sample dilution. The data obtained through super-resolution fluorescence imaging appear in excellent agreement with that obtained with TEM but with the advantage of obtaining the measurements in native solvent and allowing multi-colour imaging. Overall, this work illustrates the broad potential applicability of these techniques to the interrogation of self-assembly phenomena in organic media.

Acknowledgements

C.E.B. thanks the Bristol Chemical Synthesis Centre for Doctoral Training, funded by the EPSRC for the provision of a PhD studentship. R. F. L., P. M. and C.F.K. acknowledge grants from the EPSRC, UK (grant EP/H018301/1, EP/L015889/1) and the Medical Research Council (grant MR/K015850/1). E. M. L acknowledges the EU for a Marie Curie postdoctoral fellowship. I.M. thanks the EU for an ERC Advanced Investigator Grant which also funded a PhD studentship for J. R. F. TEM studies were carried out in the Chemistry Imaging Facility at UoB with equipment funded by UoB and EPSRC (EP/K035746/1).

Keywords: block copolymer · superresolution fluorescence microscopy · living crystallization-driven self-assembly · micelles · self-assembly

[1] A. H. Gröschel, F. H. Schacher, H. Schmalz, O. V. Borisov, E. B. Zhulina, A. Walther, A. H. E. Müller, *Nat. Commun.* **2012**, *3*, 710.
[2] Y. Mai, A. Eisenberg, *Chem. Soc. Rev.* **2012**, *41*, 5969.
[3] A.-V. Ruzette, L. Leibler, *Nat. Mater.* **2005**, *4*, 19.
[4] M. Elsabahy, K. L. Wooley, *Chem. Soc. Rev.* **2012**, *41*, 2545.
[5] Y. S. Thio, J. Wu, F. S. Bates, *Macromolecules* **2006**, *39*, 7187.
[6] F. H. Schacher, P. A. Rupar, I. Manners, *Angew. Chem. Int. Ed.* **2012**, *51*, 7898; *Angew. Chem.* **2012**, *124*, 8020.
[7] J. P. Patterson, M. P. Robin, C. Chassenieux, O. Colombani, R. K. O'Reilly, *Chem. Soc. Rev.* **2014**, *43*, 2412.
[8] M. G. L. Gustafsson, L. Shao, P. M. Carlton, C. J. R. Wang, I. N. Golubovskaya, W. Z. Cande, D. A. Agard, J. W. Sedat, *Biophys. J.* **2008**, *94*, 4957.
[9] S. W. Hell, J. Wichmann, *Opt. Lett.* **1994**, *19*, 780.
[10] T. A. Klar, S. Jakobs, M. Dyba, A. Egner, S. W. Hell, *Proc. Natl. Acad. Sci. USA* **2000**, *97*, 8206.
[11] M. J. Rust, M. Bates, X. Zhuang, *Nat. Methods* **2006**, *3*, 793.
[12] S. T. Hess, T. P. K. Girirajan, M. D. Mason, *Biophys. J.* **2006**, *91*, 4258.
[13] E. Betzig, G. H. Patterson, R. Sougrat, O. W. Lindwasser, S. Olenych, J. S. Bonifacino, M. W. Davidson, J. Lippincott-Schwartz, H. F. Hess, *Science* **2006**, *313*, 1642.
[14] M. Heilemann, S. van de Linde, M. Schüttpelz, R. Kasper, B. Seefeldt, A. Mukherjee, P. Tinnefeld, M. Sauer, *Angew. Chem. Int. Ed.* **2008**, *47*, 6172; *Angew. Chem.* **2008**, *120*, 6266.
[15] B. Huang, W. Wang, M. Bates, X. Zhuang, *Science* **2008**, *319*, 810.
[16] G. S. Kaminski Schierle, S. van de Linde, M. Erdelyi, E. K. Esbjörner, T. Klein, E. Rees, C. W. Bertoncini, C. M. Dobson, M. Sauer, C. F. Kaminski, *J. Am. Chem. Soc.* **2011**, *133*, 12902.
[17] D. Pinotsi, A. K. Buell, C. Galvagnion, C. M. Dobson, G. S. Kaminski Schierle, C. F. Kaminski, *Nano Lett.* **2014**, *14*, 339.
[18] L. Albertazzi, D. van der Zwaag, C. M. A. Leenders, R. Fitzner, R. W. van der Hofstad, E. W. Meijer, *Science* **2014**, *344*, 491.
[19] X. Wang, G. Guerin, H. Wang, Y. Wang, I. Manners, M. A. Winnik, *Science* **2007**, *317*, 644.
[20] J. B. Gilroy, T. Gädt, G. R. Whittell, L. Chabanne, J. M. Mitchels, R. M. Richardson, M. A. Winnik, I. Manners, *Nat. Chem.* **2010**, *2*, 566.
[21] P. A. Rupar, L. Chabanne, M. A. Winnik, I. Manners, *Science* **2012**, *337*, 559.
[22] H. Qiu, Z. M. Hudson, M. A. Winnik, I. Manners, *Science* **2015**, *347*, 1329.
[23] J. Schmelz, A. E. Schedl, C. Steinlein, I. Manners, H. J. Schmalz, *J. Am. Chem. Soc.* **2012**, *134*, 14217.
[24] J. Qian, X. Li, D. J. Lunn, J. Gwyther, Z. M. Hudson, E. Kynaston, P. A. Rupar, M. A. Winnik, I. Manners, *J. Am. Chem. Soc.* **2014**, *136*, 4121.
[25] L. Sun, A. Pitto-Barry, N. Kirby, T. L. Schiller, A. M. Sanchez, M. A. Dyson, J. Sloan, N. R. Wilson, R. K. O'Reilly, A. P. Dove, *Nat. Commun.* **2014**, *5*, 5746.
[26] W. Zhang, W. Jin, T. Fukushima, A. Saeki, S. Seki, T. Aida, *Science* **2011**, *334*, 340.
[27] L. Bu, T. J. Dawson, R. C. Hayward, *ACS Nano* **2015**, *9*, 1878.
[28] S. Ogi, K. Sugiyasu, S. Manna, S. Samitsu, M. Takeuchi, *Nat. Chem.* **2014**, *6*, 188.
[29] A. Pal, M. Malakoutikhah, G. Leonetti, M. Tezcan, M. Colomb-Delsuc, V. D. Nguyen, J. van der Gucht, S. Otto, *Angew. Chem. Int. Ed.* **2015**, *54*, 7852; *Angew. Chem.* **2015**, *127*, 7963.
[30] M. E. Robinson, D. J. Lunn, A. Nazemi, G. R. Whittell, L. De Cola, I. Manners, *Chem. Commun.* **2015**, *51*, 15921.
[31] S. Ogi, V. Stepanenko, K. Sugiyasu, M. Takeuchi, F. Würthner, *J. Am. Chem. Soc.* **2015**, *137*, 3300.
[32] K. Kolmakov, C. A. Wurm, D. N. H. Meineke, F. Göttfert, V. P. Boyarskiy, V. N. Belov, S. W. Hell, *Chem. Eur. J.* **2014**, *20*, 146.
[33] V. N. Belov, G. Y. Mitronova, M. L. Bossi, V. P. Boyarskiy, E. Hebisch, C. Geisler, K. Kolmakov, C. A. Wurm, K. I. Willig, S. W. Hell, *Chem. Eur. J.* **2014**, *20*, 13162.
[34] Z. M. Hudson, C. E. Boott, M. E. Robinson, P. A. Rupar, M. A. Winnik, I. Manners, *Nat. Chem.* **2014**, *6*, 893.

Received: October 13, 2015
Published online on November 10, 2015

